Awanui Artesian Aquifer

AWANUI ARTESIAN AQUIFER
NUMERICAL MODELLING

- Final
- 22 March 2007

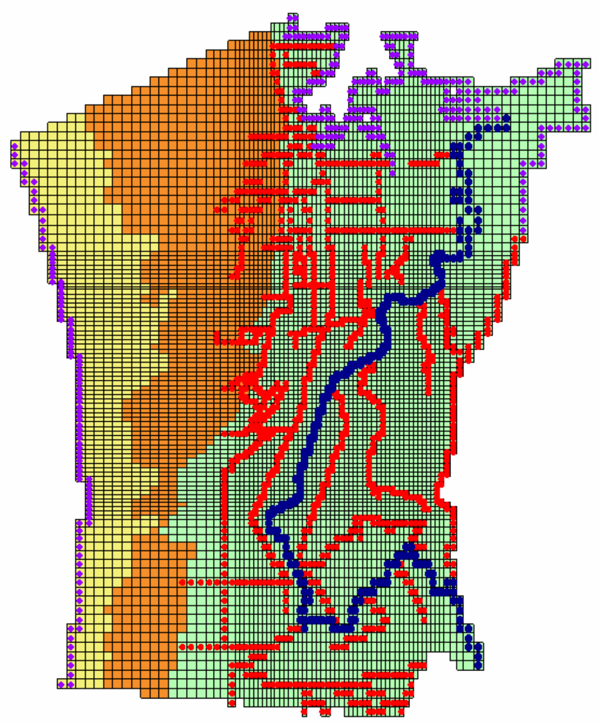

Awanui Artesian Aquifer

AWANUI ARTESIAN AQUIFER NUMERICAL MODELLING

- Final
- 22 March 2007

Sinclair Knight Merz
25 Teed Street
PO Box 9806
Newmarket, Auckland New Zealand
Tel: +64 9 913 8900
Fax: +64 9 913 8901
Web: www.skmconsulting.com

Contents

SKM

Document history and status

Revision	Date issued	Reviewed by	Approved by	Date approved	Revision type
Draft A	14 Feb 2007	BNH, JLW	Jon Williamson	13 Feb 2007	Draft for client review
Final	22 Mar 2007	Ken MacKenzie	Jon Williamson	22 Mar 2007	Client comments and final QA

Distribution of copies

Revision	Copy no	Quantity	Issued to
Draft A	1	1	Northland Regional Council
Final	1 – 3	3	Northland Regional Council
Final	4 – 5	2	SKM Auckland

Printed:	22 March 2007
Last saved:	22 March 2007 11:39 AM
File name:	I:\Aenv\Projects\AE02527\Reports\Awanui_Numerical Modelling Report_FINAL.doc
Author:	Blair Thornburrow
Project manager:	Ken MacKenzie
Name of organisation:	Northland Regional Council
Name of project:	Awanui Artesian Aquifer
Name of document:	Awanui Artesian Aquifer - Stage 2 Numerical Modelling
Document version:	Final
Project number:	AE02527

1. Introduction

1.1 Background

The Northland Regional Council (NRC) commissioned Sinclair Knight Merz (SKM) to undertake hydrogeological investigations and groundwater modelling of the Awanui artesian aquifer to assess the effects of progressive closure of abandoned flowing artesian bores in the Awanui area. The study area is shown in Figure 1. The first stage of the investigation comprised collation of available hydrogeological data in a report providing a conceptualisation of aquifer hydrogeology (SKM, 2006). The hydrogeological conceptualisation report forms the basis for development of the numerical groundwater model detailed in this report.

- **Figure 1. Site Basemap.**

  (See A3 attachment at rear).

1.2 Previous Modelling

The modelling in this project is based in part on previous modelling work undertaken in the Aupouri Peninsula, north of Awanui by HydroGeo Solutions (2000). While the previous model focussed on a zone generally outside the current study area, elements of the model such as aquifer hydraulic properties and recharge characteristics were utilised as a basis for the development of the current model.

1.3 Objectives

The main objectives of this modelling project are to:

1) characterise the hydrogeological system and represent it via numerical modelling, and;
2) identify and describe the potential effects on the aquifer of progressively capping abandoned flowing artesian bores.

SKM

2. Aquifer Conceptualisation

This section summarises the main findings from the stage one hydrogeological conceptualisation report (SKM, 2006) and presents them in terms of how they are applied to the numerical groundwater model.

2.1 Geological Units

A number of geological units have been differentiated and are summarised in Table 1. Units are listed in typical stratigraphic depth order.

- **Table 1. Model geological units.**

Name	Q map unit(s)	Description
Loose dune sand	Q1d – Kariotahi group	Loose sand in mobile dunes. Highly permeable. Holocene age.
Weathered dune sand	eQd – Kariotahi group	Partially or weakly cemented Pleistocene dune sand.
Alluvium	Q1a – Kariotahi group	Interbedded sand, peat, mud, gravel and clay deposits. Holocene to Pleistocene age.
Peat and sand	eQd – Kariotahi group	Interbedded peats and sands causing vertical confinement in dune areas. Pleistocene age.
Fine sand	Q1a – Kariotahi group	Fine quaternary sands near west coast underlying units above. Pleistocene age.
Shell bed	Q1a – Kariotahi group	Shell bed overlying bedrock. Highly permeable unit with areas of artesian pressures. Pleistocene age.

The sedimentary basement is not included as a model geological unit as it defines model extent represented by a no flow boundary. A no flow boundary is assigned here due to the sharp conductivity gradient encountered at the interface between loose sediments and basement rock.

- **Figure 2. Geology map.**

(See A3 attachment at rear.)

2.2 Aquifer Recharge

Recharge to groundwater is the flux of water to the water table. Recharge rates vary depending on characteristics of rainfall, lithology, vegetation, topography (and others).

2.2.1 Background

In the Northland region, sand aquifers account for 5 to >50% of annual rainfall and hard rock aquifers recharge may be 0 to 10% of annual rainfall (HydroGeo Solutions, 2000). This is primarily due to variations in permeability where sand aquifers are able to drain significant volumes of rainwater. Evidence of this is seen in the reduced amount of surface runoff and evaporation in sand dominated lithologies.

In the model domain groundwater recharge forms a major component of the aquifer water balance. The primary difference in recharge regimes between sand and alluvium is that the rate of infiltration to groundwater is significantly higher for sand than for alluvium. Numerous lakes occur within the sand dunes in the west of the model domain. These features perch water above low permeability lacustrine sediments and cause slow and attenuated recharge to groundwater. Average recharge is lower here due to of evaporative losses from the lakes.

2.2.2 Estimating Recharge

The process of determining recharge to the model was carried out using a Soil Moisture Water Balance Model (SMWBM). Three separate zones of recharge behaviour were defined within the western dune sands and the alluvial plains (Figure 3) each possessing unique water balance characteristics (Figure 4).

Since no stream flow data were available to calibrate the SMWBM directly, parameters were adjusted based on conceptual understanding, previous modelling work and as part of the transient calibration process of the groundwater model. Details of recharge estimation are provided in Appendix A. Groundwater recharge is estimated by the SMWBM as 43.7% and 4.2% of the average annual rainfall in the dune sand and alluvial plains respectively.

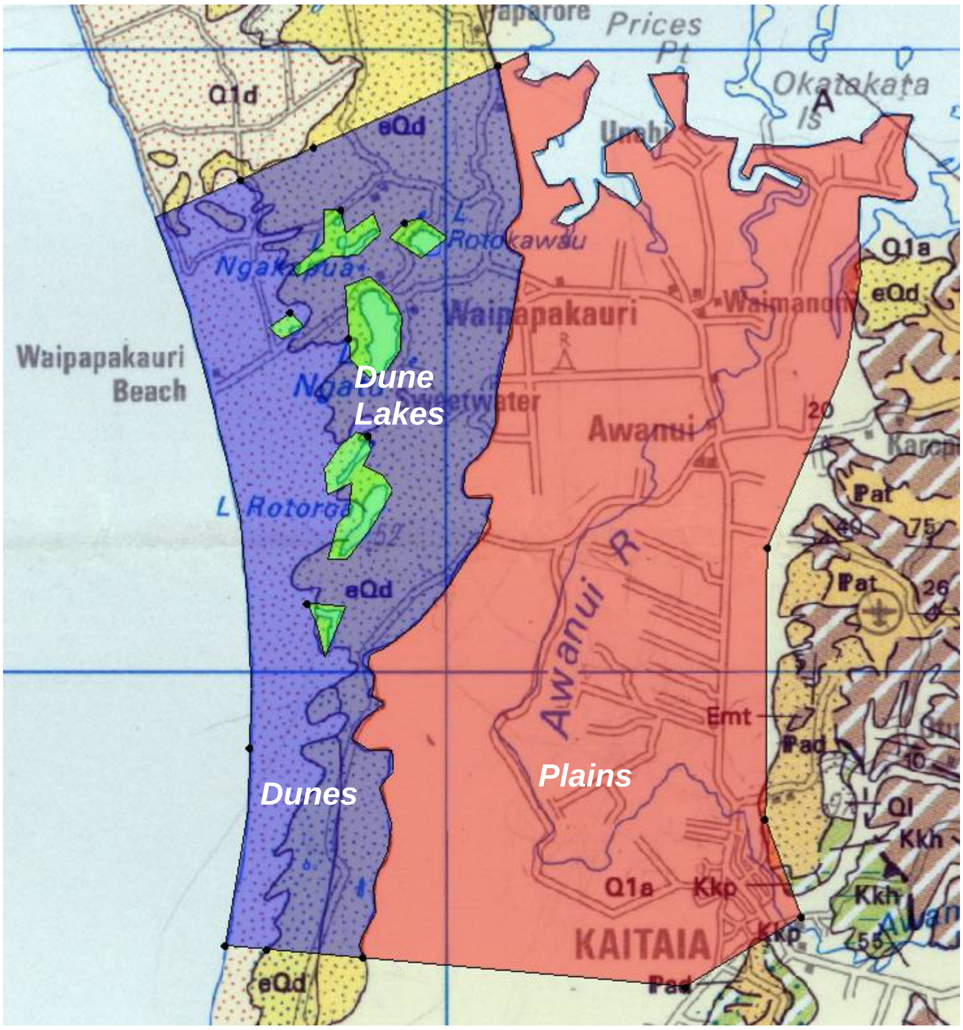

▪ **Figure 3. Model recharge coverages.**

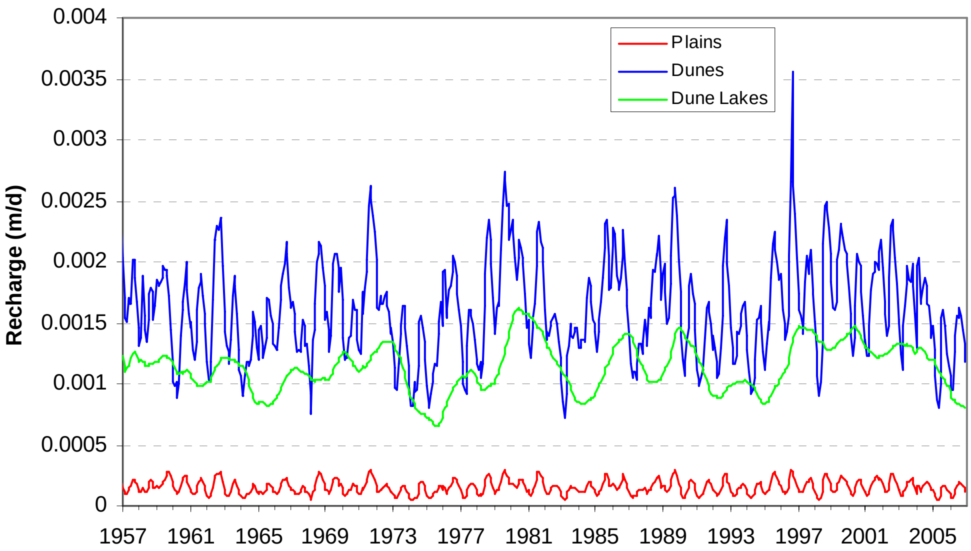

- **Figure 4. Simulated transient recharge.**

Recharge from the dune lakes was modelled as a separate recharge coverage to represent the unique hydrological characteristics of these features. Impermeable lake bed sediments partially isolate lake waters from the underlying groundwater system. As a result, although there is some degree of leakage through the lake bed sediments, it is typically slow and attenuated when compared with direct recharge through dune sands.

In order to simulate the recharge time series from the dune lakes the calculated recharge for the dune area was smoothed and delayed via a preceding 2-year moving average to simulate the delayed response caused by slow leakage through lake bed sediments. A 30% reduction to total recharge was then applied to account for evaporative losses from the dune lakes (Figure 4). It should be noted that this method provides an approximate estimate from the dune lakes only as it is not in the scope of the project to examine the dune lake groundwater regime in detail. However, the procedure outlined creates a groundwater response that matches well to observed groundwater level variations. Overall the small area within the dune lake recharge coverage means that the model is relatively insensitive to lake recharge characteristics.

2.3 Drainage

While the zone of sand dunes near the west coast is relatively free of surface water drainage features, the low lying Awanui Plains have an extensive drainage network and include the lower reaches of the Awanui River (Figure 1). Drains carry runoff created by excess infiltration during rainfall events as well as baseflow derived from drainage of groundwater from the surrounding unconfined aquifer.

The drains that cross the alluvial plains were formed to drain the low lying plains area to increase productivity. Due to the location of the historic flowing artesian bores it is thought that some of the drains were specifically installed to carry water from the free flowing artesian bores. Therefore the number of existing drains does not necessarily relate to flood prevalence in the plains.

2.4 Aquifer Hydraulic Properties

Initial model hydraulic parameters were derived from previous modelling described in HydroGeo Solutions (2000). Initial parameter estimates were then refined during the calibration process. The final model parameters adopted for this model in part reflect the relative complexity of the vertical layer subdivision applied to simulate artesian conditions and hydrogeological unit differentiation compared to the previous model application, which was a simple single layer model.

2.5 Piezometric Surface Geometry

A generalised regional piezometric contour map based on interpolated topography and bore log water level information was developed in SKM (2006) and is shown in Figure 5. A groundwater flow divide is demonstrated along the centre of the dune ridge, mimicking topography and separating groundwater flows west to the coast and east to the Awanui Plains. Groundwater flows in the flood plain area generally conform to the surface drainage with overall drainage into the Rangaunu Harbour.

- **Figure 5. Regional piezometric contour map.**

  (See A3 attachment at rear).

2.6 Groundwater Level Monitoring

There are eight monitoring sites within the model domain of which five had sufficient records for transient calibration. Their locations are shown in Figure 6 and details of bore location and depth are provided in Table 2.

- **Table 2. Monitoring bore details.**

Site Name		Site Number	Easting (m NZMG)	Northing (m NZMG)	Ground (mAMSL)	Bore depth (m)	Welarc ID
Lake Heather No.1	deep	5301003	2528400	6683500	31.65	105.5	226
	mid					62	
	shallow					29	
Lake Heather No.2		5301005	2528292	6683585	35.75	30	227
Lake Heather No.3		5301007	2528419	6683686	33.4	29	228
Ogle Drive[1]		5301001	2528577	6689660	35.65	69	81
Crene		5322001	2533500	6679500	6.5*	29	1037
Sweetwaters[2]		5322003	2531300	6684600	3.98	34	1025
Matich[2]		5302003	2531300	6685800	?	?	?
Shanks[2]		5322005	2534200	6679300	?	?	?

[1]Bore outside model domain, but compared to nearest model location; [2]Insufficient data for transient calibration.
*Interpolated from LIDAR data.

- **Figure 6. Groundwater monitoring locations.**

(See A3 attachment at rear).

Hydrographs for the three piezometers at Lake Heather are shown in Figure 7. This site corresponds to the best groundwater level data record in the model domain, with a nested piezometer demonstrating vertical confinement. The records extend from 1988 to 2005 and data frequency is approximately monthly.

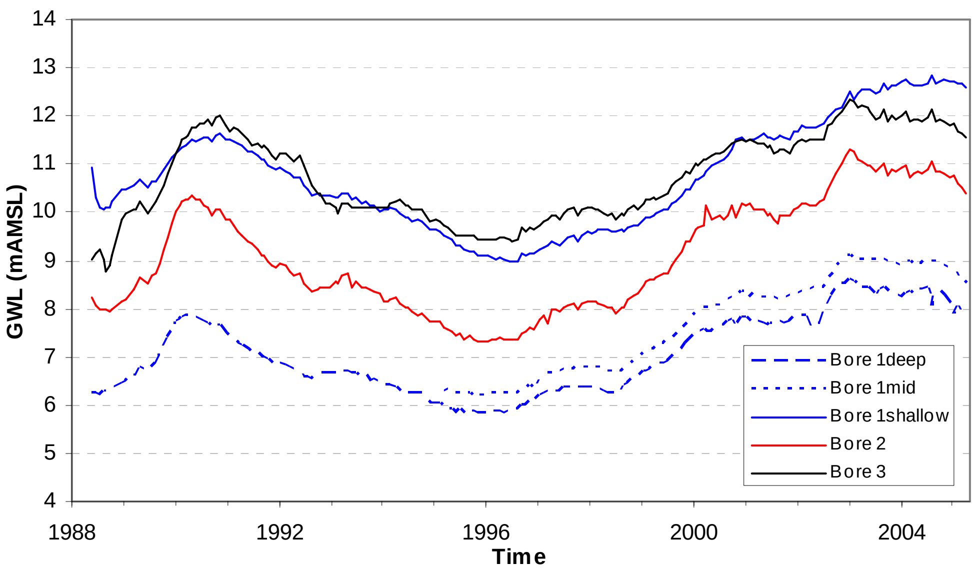

- **Figure 7. Lake Heather bores hydrograph.**

The Crene bore has the only reliable record available in the Awanui Plains and extends from 1994 to 2005 (Figure 8). This record appears to be influenced by pumping, and it is suggested in the drillers log that this is a monitoring piezometer for an adjacent pumping bore. This was taken into account during transient calibration to these data.

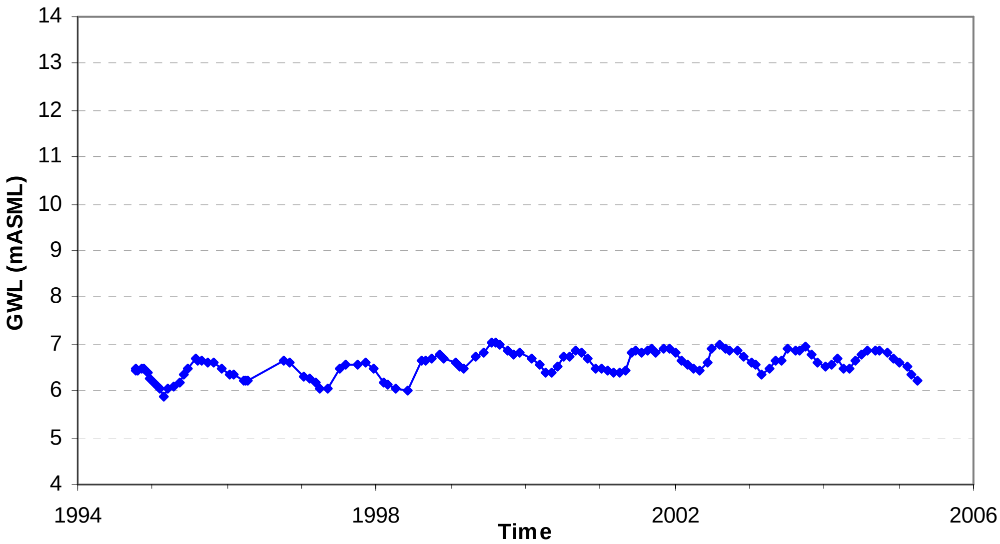

▪ **Figure 8. Crene bore hydrograph.**

The data record for the bore at Ogle Drive, Paparore is shown in Figure 9. This bore lies approximately 1 km north of the model boundary in the sand dune zone. This record was used to provide a comparison with computed heads at the nearest point in the model, however precise calibration was not sought due to its location outside the model domain.

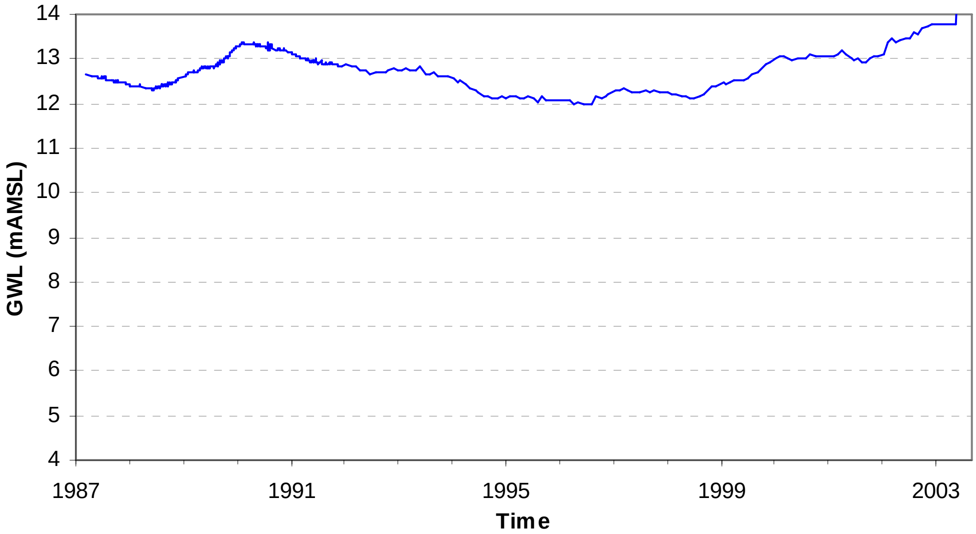

■ **Figure 9. Ogle Drive bore hydrograph.**

3. Model Configuration

The MODFLOW 2000 code developed by U.S.G.S. with the GMS 6.0 modelling environment is used to construct models and run simulations in this study.

3.1 Model Domain

The model consists of 27,974 active cells over four layers representing the geological structure of the Awanui Plain and coastal dunes. Plan-view cell dimensions vary from 200 × 200 m and are refined to 100 × 100 m in the zone of interest. The overall area of the model domain is approximately 118 km^2. Figure 10 shows the model grid.

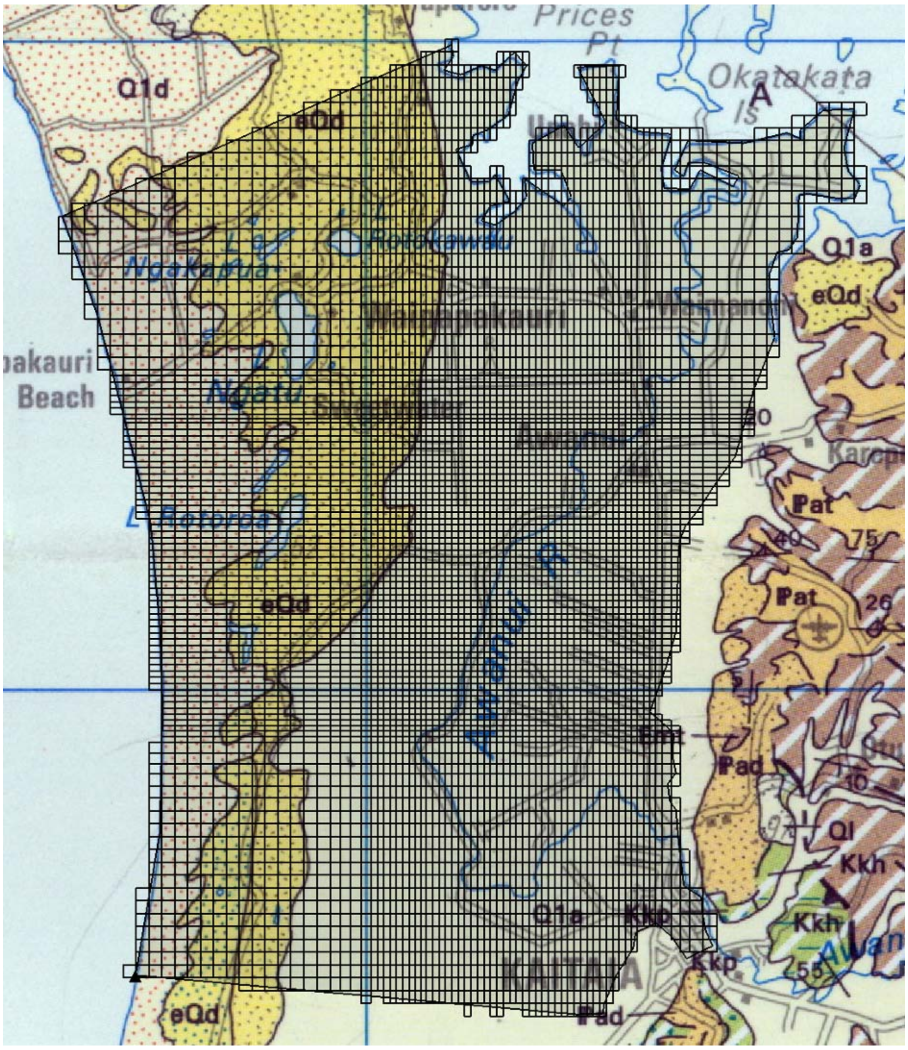

- **Figure 10. Awanui model grid (layer 1).**

3.2 Boundary Conditions

The boundary conditions defined in this model include no flow, constant head, drain and river boundaries. Boundary conditions are shown in terms of the model grid in Figure 11.

3.2.1 Constant Head Boundaries

Constant head boundaries in this model are defined along the coast to simulate sea level pressures along the western model boundary and across Rangaunu Harbour. Groundwater elevation in these cells is set to 0 mAMSL to reflect mean sea level allowing the model to simulate natural groundwater flow to the coast.

3.2.2 River Boundaries

The Awanui River is represented by a river boundary which allows the model to replicate the interaction between the river and adjacent unconfined aquifer system. River bed and stage height elevations are interpolated from a LIDAR scan of the flood plain and a bed conductance assigned to represent the degree of hydraulic connection between the river and adjacent aquifer system.

SKM

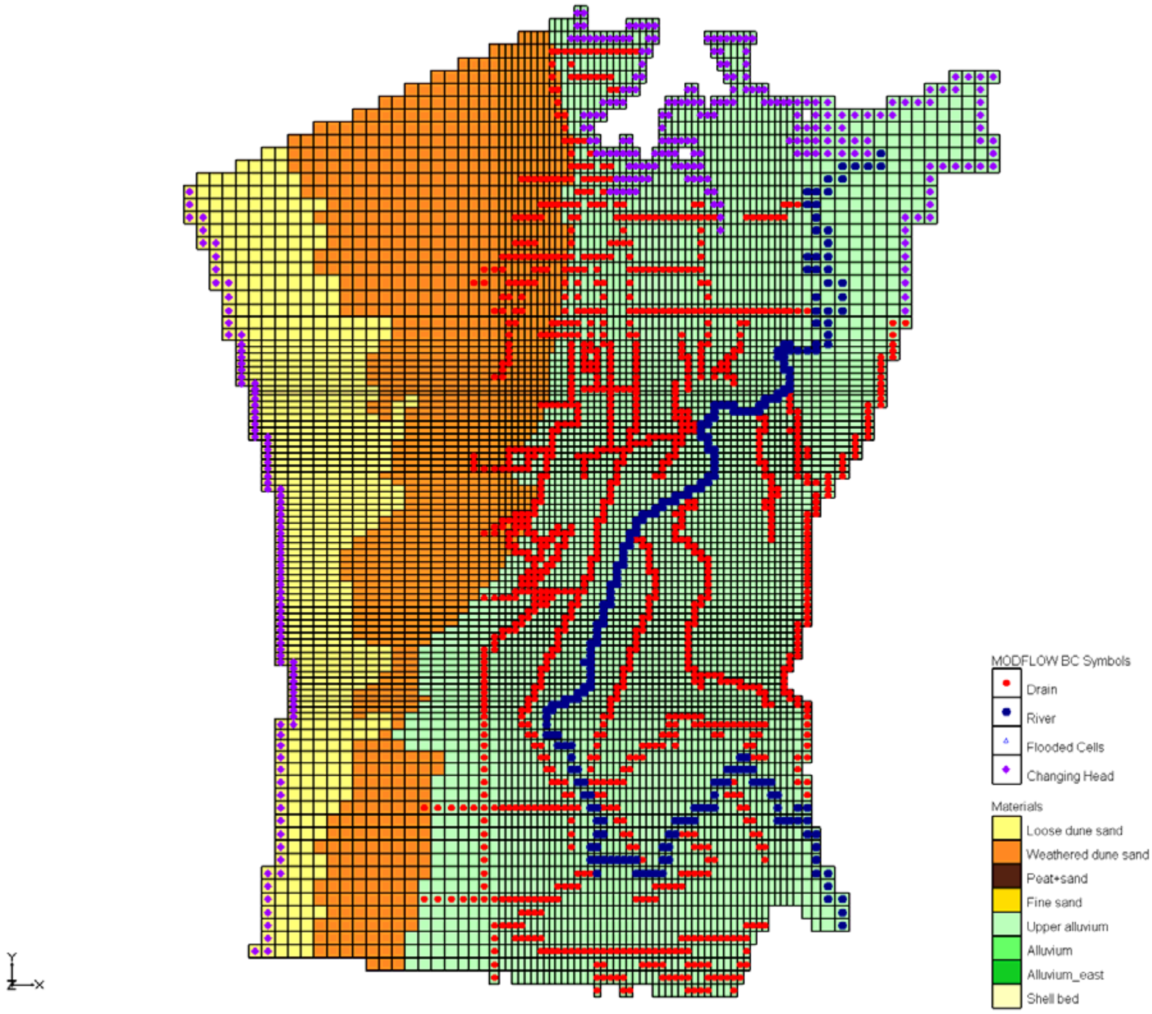

- **Figure 11. Model boundary conditions (layer 1).**

3.2.3 Drain Boundaries

Drain boundaries replicate the drainage of water from an unconfined aquifer to a natural or artificial drainage feature. The extensive surface drainage network in the Awanui Plain is represented by a number of drain boundaries. Each drain cell has a defined bed elevation (based on interpolated topography) and is assigned a conductance value reflecting the drain's ability to remove water from the aquifer which is assumed to have little restriction in this area. Water is removed from the model when groundwater levels exceed the nominated bed elevations.

In order to simulate the effect of free flowing artesian bores drain boundaries were situated in the bottom model layer. These boundaries were established to remove water from layer four of the model when piezometric head exceeds ground elevation. In order to represent bore efficiency a conductance term was assigned to each cell. This conductance term was scaled such that a realistic magnitude of flow from the artesian bores is simulated, based on available observations. The drain conductance used for artesian bores is 30 m^2/day.

Very limited data were available in terms of the quantity, layout and discharge of artesian bores, however a synthetic distribution provided by NRC comprising 107 bores was used (Figure 12). This extrapolated data set was created based on local knowledge of bore locations relative to surface drains and farm layout. Due to the limited information available on the location of existing free-flowing artesian bores the total amount of artesian flow can not be accurately estimated. However, the relative effects of bore closure are still able to be examined based on the nominal bore locations used.

- **Figure 12. Synthetic distribution of flowing artesian bores.**

  (See A3 attachment at rear.)

3.2.4 No Flow Boundaries

The southern, northern and eastern inland limits of the model are all represented by no flow boundaries. The northern boundary dissects the sand ridge perpendicular to expected regional flow pattern, so is considered not to affect model behaviour. The eastern boundary lies at the boundary of the relatively impermeable sandstone/mudstone hills except for where the Awanui River enters the model domain. While the southern no flow boundary may interrupt expected groundwater flows into or out of the model domain, this has been extended south away from the zone of interest such that its influence will be insignificant to the model application in the focus area of the study. At the base of the model, a no flow boundary represents the interface between sediments and basement rock.

3.3 Model Layer Configuration

3.3.1 Layer Geology

The four model layers have been divided into material zones in order to best represent the conceptualised geological structure within the model domain. Figure 13 shows the geological subdivision for each model layer.

3.3.2 Layer Elevations

The vertical boundaries between each model layer have been determined based on bore log information and hydrogeological cross sections developed in SKM (2006). Surfaces for layer boundaries were interpolated from a combination of drillers' depth logs and interpolated ground level for each bore location. Rules were applied such that layer boundary surfaces did not overlap and unit termination was adequately represented. Model layer elevation contour maps for each boundary are supplied in Appendix B. 3D orthographic views of the model layer configuration are shown in Figure 13, illustrating the relief of each layer boundary.

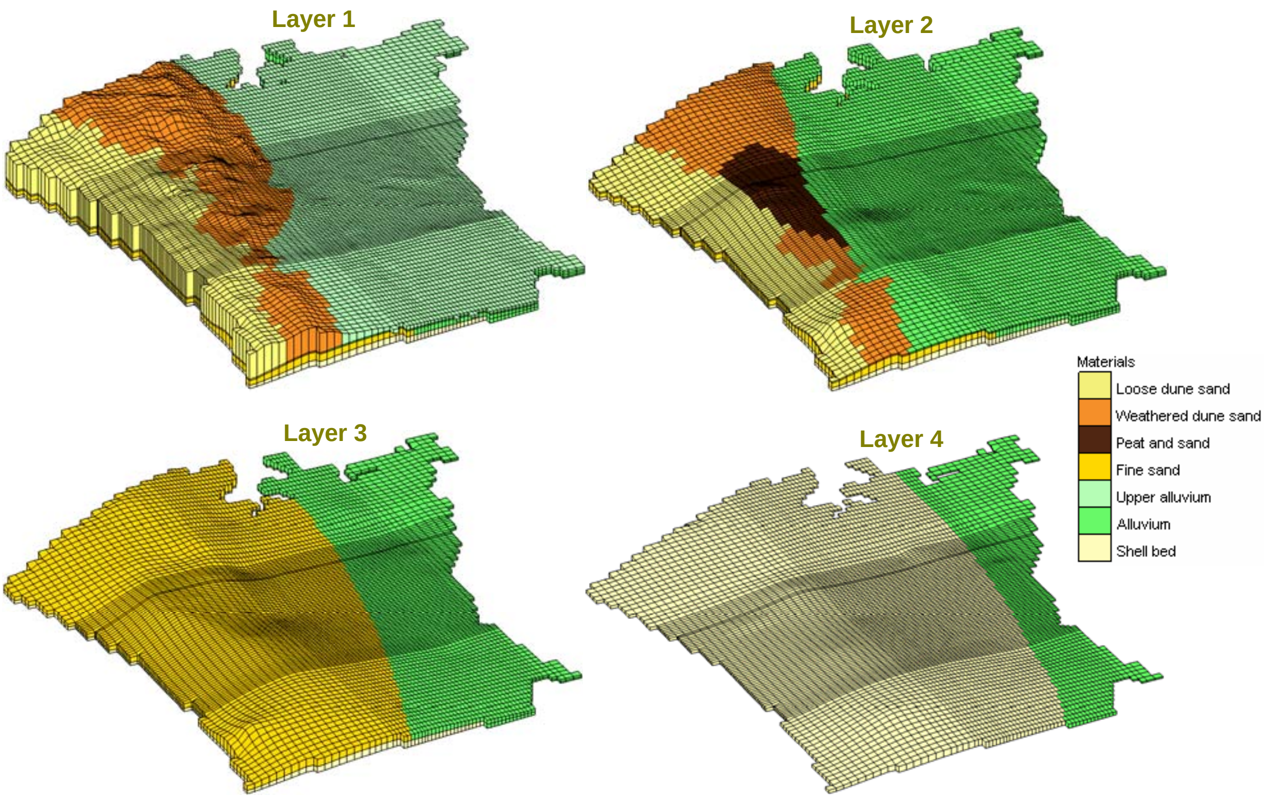

■ **Figure 13. 3D orthographic views of model layer configuration.**

4. Model Calibration

Calibration of the numerical groundwater model was achieved by manual adjustment of model parameters to provide a best fit with nominated calibration targets. The calibration process is detailed in the following sections.

4.1 Steady State Calibration

In order to obtain approximate model parameters and verify the validity of hydrogeological conceptualisation, an initial process of steady state calibration was employed. Once a satisfactory calibration was established, steady state heads were used to define the initial starting condition for the transient calibration process.

Measured water levels from drillers' borelogs were used as steady state observed heads. The variable reliability of these records, as well as uncertainty brought about by poorly defined topographic reference and varying timing of measurement meant that steady state calibration was limited. Because of these reasons, little effort was spent trying to improve the steady state calibration. If sufficient data is available, transient calibration provides a far more powerful and representative method of model parameterisation.

4.2 Transient Calibration

Following initial steady state calibration, transient calibration was undertaken. This process involved running the model through iterations of time and comparing time series results to groundwater monitoring records, which provided an opportunity to improve model calibration. Due to the limited reliability of steady state observation data, a majority of the parameterisation process was undertaken during the transient model calibration.

4.2.1 Stress Periods and Time Steps

The length of reliable rainfall data available to model transient recharge determined the maximum length of calibration model run. Adequate rainfall data spanned a 52 year period from 1955 to 2007. All available groundwater level records occur within the years 1987 to 2007, during which period reliable rainfall data was available.

Monthly stress periods were chosen to create a level of temporal resolution most similar to that of the observation data. A 50 year model run period (spanning 1957 to 2007) was used so that subsequent predictive scenarios could be accommodated. There were 600 stress periods used in the transient calibration model each having 3 time steps with a multiplier of 1.2. Run times during transient calibration were typically around five minutes.

SKM

4.2.2 Initial Conditions

Starting heads for the transient calibration were initially set to output head values from the steady state model. During the process of transient calibration, heads from discreet time steps of the calibration runs were used to define initial conditions. This was carried out so that conditions matching the likely climatic situation at the start of the calibration time were used.

4.2.3 Model Parameters

Calibrated model parameters for the geological units shown in Figure 13 are provided in Table 3.

- **Table 3. Calibrated model parameters.**

Material ID	K_h (m/d)	K_h (m/s)	Vertical anisotropy	S_y
Loose dunesand	10	1.2e-4	10	0.2
Weathered dunesand	6	6.9e-5	10	0.2
Fine sand	3	3.5e-5	25	0.25
Peat and sand	0.1	1.2e-6	30	0.2
Upper alluvium	0.55	6.4e-6	10	0.3
Alluvium	0.06	6.9e-7	20	0.05
Shell bed	50	5.8e-4	2	0.3

4.2.4 Calibration to Observed Heads

Groundwater monitoring records as provided in Section 2.6 were used to calibrate the transient groundwater model. Measured and modelled transient heads from two (shallow and deep) Lake Heather bores in the western sand dunes are plotted in Figure 14. The timing and magnitude of groundwater level fluctuations is matched moderately well by the model, while a similar downwards pressure gradient is simulated. Site specific characteristics such as the influence of multiple confining layers throughout the lithological profile are likely responsible for some of the disparity between modelled and observed fluctuations.

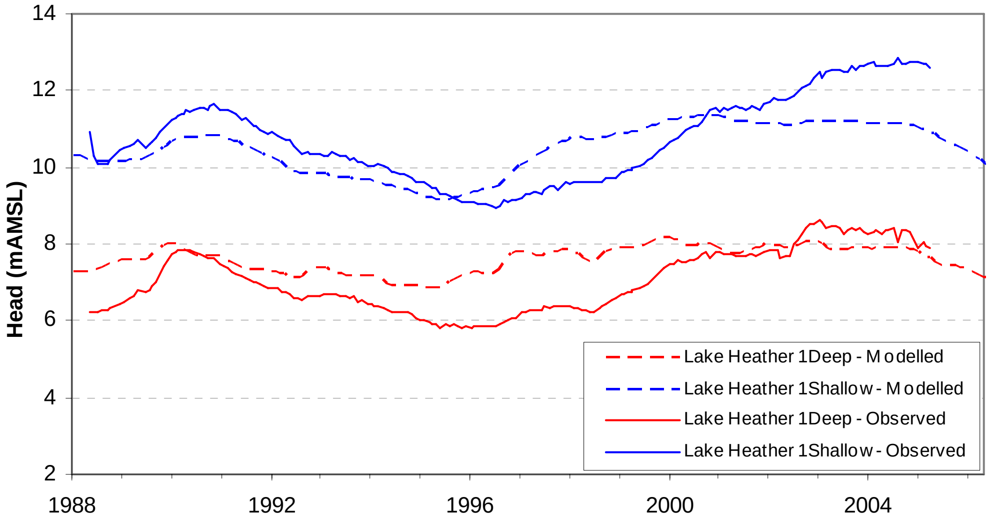

▪ **Figure 14. Modelled and observed heads at the Lake Heather monitoring site.**

Measured and modelled heads from the Crene bore situated on the Awanui Plain are plotted in Figure 15. Modelled data beyond 1999 match more closely to observations and this may be due to pumping prior to that time (refer to Section 2.6). This is evident in the nature of groundwater level fluctuations, which appear to show drawdown and recovery events. Overall, piezometric response in the model appears to be well calibrated in this location.

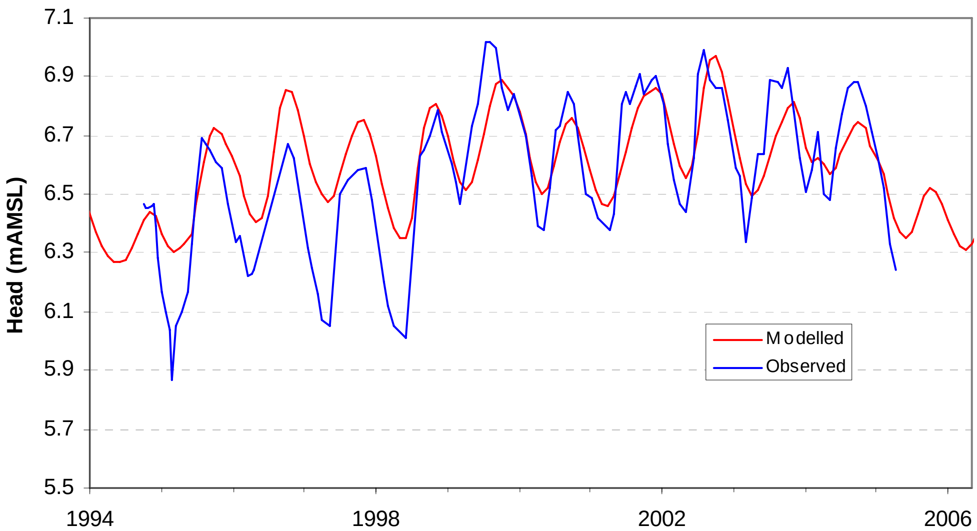

▪ **Figure 15. Modelled and observed heads at Crene bore.**

Figure 16 presents measured heads from the Ogle Drive bore, situated north of and outside the model domain and simulated heads in the nearest model cell. The offset between modelled and observed head reflects the relative difference in topographic elevation between these points however the timing and magnitude of head fluctuations is matched well.

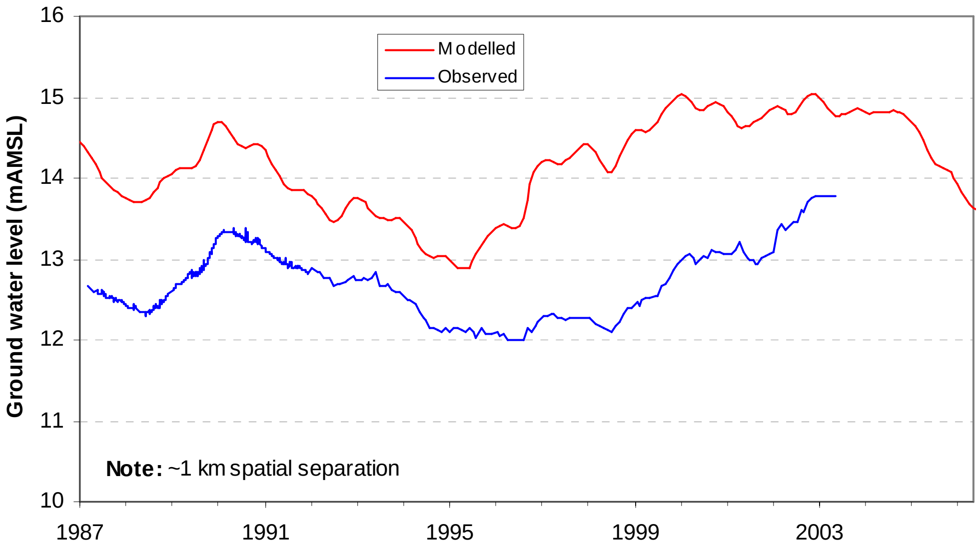

- **Figure 16. Modelled and observed heads at Ogle Drive bore.**

The Root Mean Squared (RMS) error of this calibration calculated from the Lake Heather and Crene bores (Figure 14 and Figure 16) is 0.73 m. This equates to 9.4% of the range of observed transient heads across the model domain.

Due to the limited amount of available calibration data, the complete datasets were used for calibration as opposed to holding an amount of data for verification purposes.

4.3 Calibrated Model Outputs

4.3.1 Piezometric Surface Geometry

An example piezometric surface map during winter 2000 for layer 1 of the calibrated model is shown in Figure 17. As previously discussed in the hydrogeological conceptualisation report (SKM, 2006), a ridge of higher water table elevation coincides with the dune ridge and acts as a groundwater flow divide to the east and west.

Water table geometry in the alluvial plains is dominated by drainage features, between which the water table becomes mounded. In reality, the degree of water table mounding shown in the model exceeds ground surface elevation and would not occur, but instead increased surface runoff would result. The MODFLOW environment does not take into account ground elevation thus does not remove water above the ground surface. The presence of flooded cells does indicate however that the plains are likely to experience a degree of groundwater discharge and excess surface water runoff. The fact that the actual drainage network is denser and more complex than in the model also contributes to this effect. Due to the model grid resolution, definition of the complete drainage network would lead to the model becoming over-constrained.

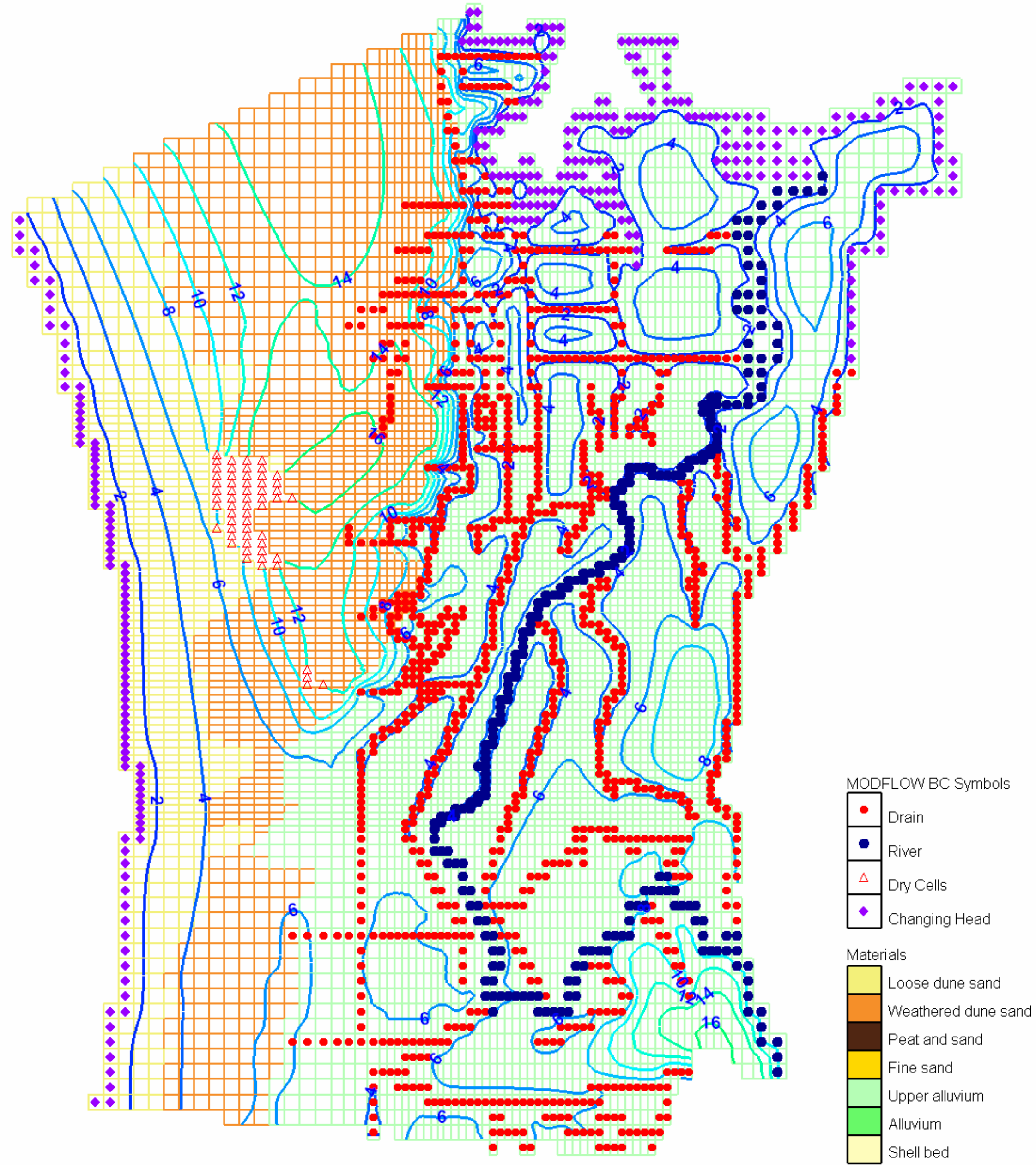

▪ **Figure 17. Piezometric surface map (mAMSL) during wet conditions.**

4.3.2 Model Flow Budgets

The average flow budget for the calibrated model is summarised in Table 4, which provides flow rates to and from the model domain as average values over the model run period. Rainfall recharge is by far the main input of water into the model accounting for 99.8% of total inflows while a very small amount of water is leaked from the Awanui River. Flux out of the model domain is accounted for by flow to coastal constant head cells, surficial drain cells, artesian bore drain cells and river cells. Constant head cells representing the coast are the largest component of outflow and account for 68.2% of total model discharge. Surficial drain cells, predominantly in the Awanui Plain are responsible for 23.1% of outflows and artesian bores and river cells account for 5.9% and 2.7% of outflows respectively.

- **Table 4. Average flow budget for calibrated transient model.**

Component	Flow (m^3/day)	Proportion of flow (%)
FLOW IN		
Recharge	81,917	99.8
Rivers	115	0.14
Net change in storage	76	0.09
Constant heads	0	0
TOTAL IN	**82,108**	**100**
FLOW OUT		
Constant heads	-56,058	68.2
Drains	-18,991	32.1
Artesian bores	-4,865	5.9
Rivers	-2,193	2.7
TOTAL OUT	**-82,108**	**100**

Note: Change in storage is due to difference in conditions between start and end of model run.

A time series plot of the above flow budget components is presented as Figure 18. Inflows to model cells are plotted as positive values while losses are negative.

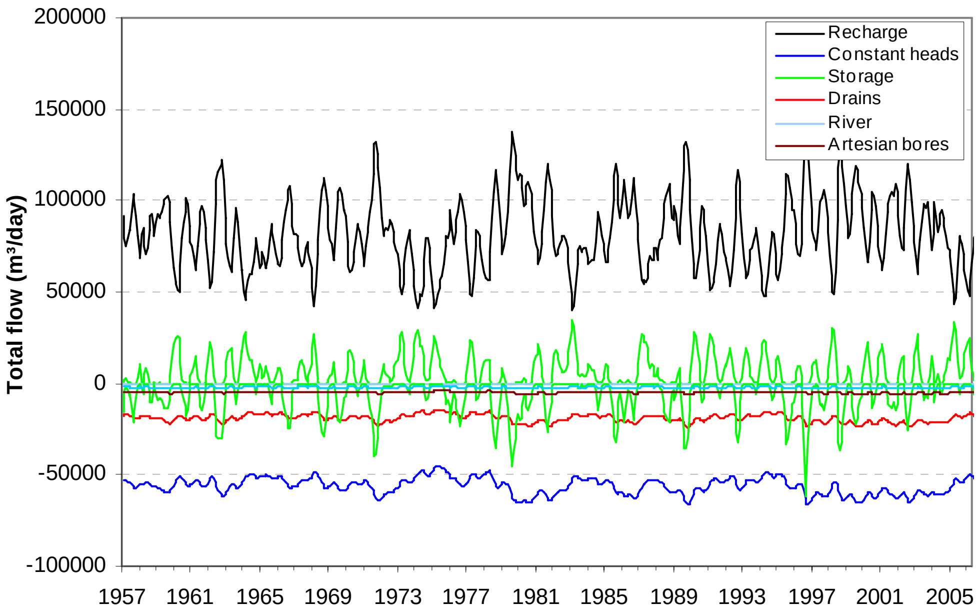

- **Figure 18. Time series flow budget for calibrated model.**

Figure 19 shows the calibrated groundwater model flow budget in terms of the dune and alluvial plain zones, and averaged over time to eliminate storage effects. Recharge to groundwater in the plains accounts for just 14% of the total model recharge due to differing soil properties (see Section 2.2). Of the 70,800 m^3/d of recharge to the dune zone, 84% is discharged to the Tasman Sea and to surface drainage. This is the most significant discharge point in the model due to it receiving the majority of recharge from the highly permeable dune zone. The remaining 11,300 m^3/d (16% of recharge) is transmitted from the dune zone into the alluvial plains zone, primarily via the higher permeability underlying shell and sand deposits. Confinement due to the lower permeability alluvial sediments above means artesian pressures are generated. Subsequently, 4,900 m^3/d of groundwater is removed via the arbitrary artesian bores across the plains.

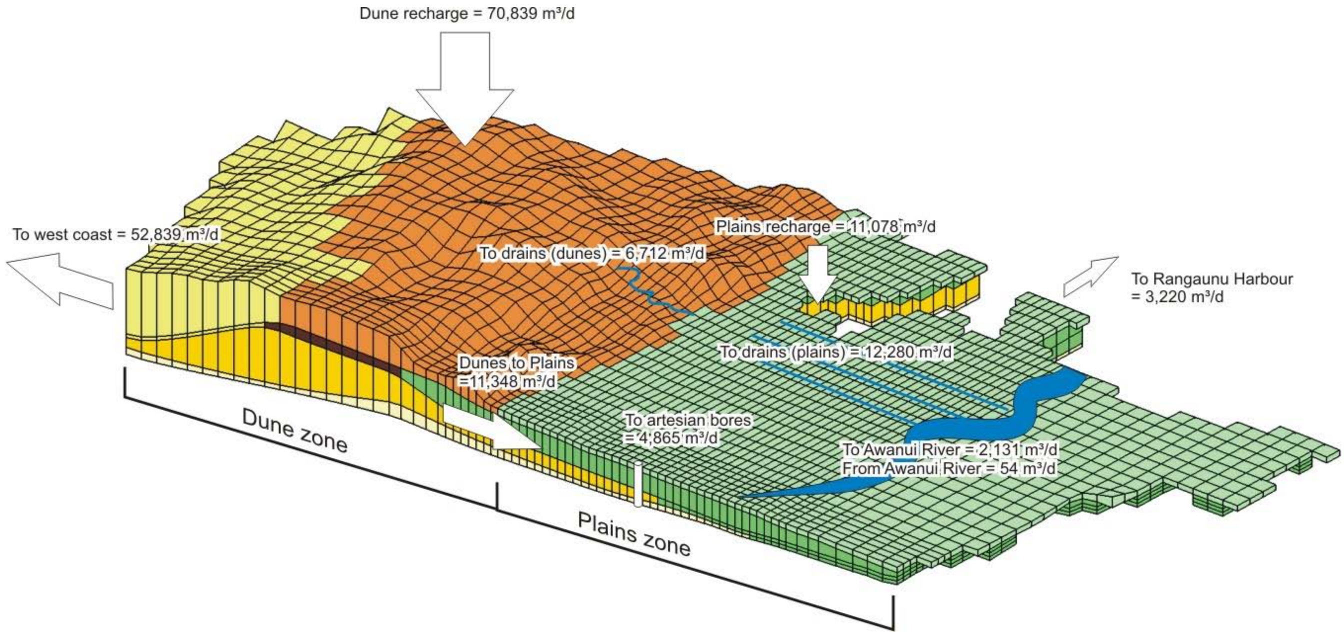

- **Figure 19. Schematic diagram of zonated model flow budget for calibrated model[1].**

4.3.3 Free Flowing Artesian Bores

Total simulated flow from the synthetic artesian borefield is presented in Figure 20. Seasonal fluctuations in discharge reflecting recharge in the plains overlie interannual fluctuations relating to groundwater pressures in the shell bed. Variability is low, with the range in flows accounting for about 30% of the mean. It should be noted that due to the lack of data relating to the quantity, spatial distribution and flow of artesian bores, these results are indicative and for comparison purposes only until further data are available.

---

[1] Note that flow rates differ from Table 4 due to zone subdivision of the flow budget.

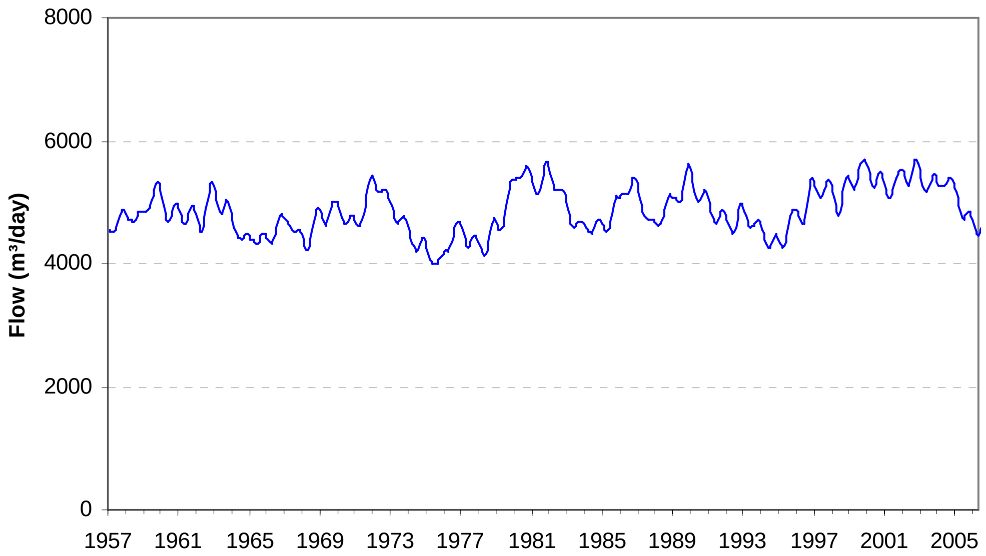

Figure 20. Combined flow from synthetic artesian borefield in calibrated model.

4.4 Sensitivity Analysis

A sensitivity analysis was carried out on the calibrated model to demonstrate the effects of higher and lower values of hydraulic conductivity (K) on model calibration hydrographs. During the calibration process, conductivity was identified as being the most sensitive parameter. K values are doubled across the model for the first scenario and halved for the second. Findings are presented in the following sections.

4.4.1 Scenario 1: 100% increase in K

Scenario 1 of the sensitivity analysis assesses the effect on calibration of increasing the hydraulic conductivity across the whole model by 100% (i.e. doubling K). Doubled horizontal hydraulic conductivities used in this scenario are provided in Table 5. Vertical hydraulic conductivity is determined by the anisotropy factor specified in Table 3.

Table 5. Hydraulic conductivity (K) values used for sensitivity analysis scenario 1.

Material ID	K_h (m/d)	K_h (m/s)
Loose dunesand	20	2.4e-4
Weathered dunesand	12	1.4e-4
Fine sand	6	7.0e-5
Peat and sand	0.2	2.4e-6
Upper alluvium	1.1	1.3e-5
Alluvium	0.12	1.4e-6
Shell bed	100	1.2e-3

Figure 21 shows the effect on the Lake Heather bores calibration time series. Magnitude and variability of hydraulic head has decreased significantly as well as the degree of vertical confinement.

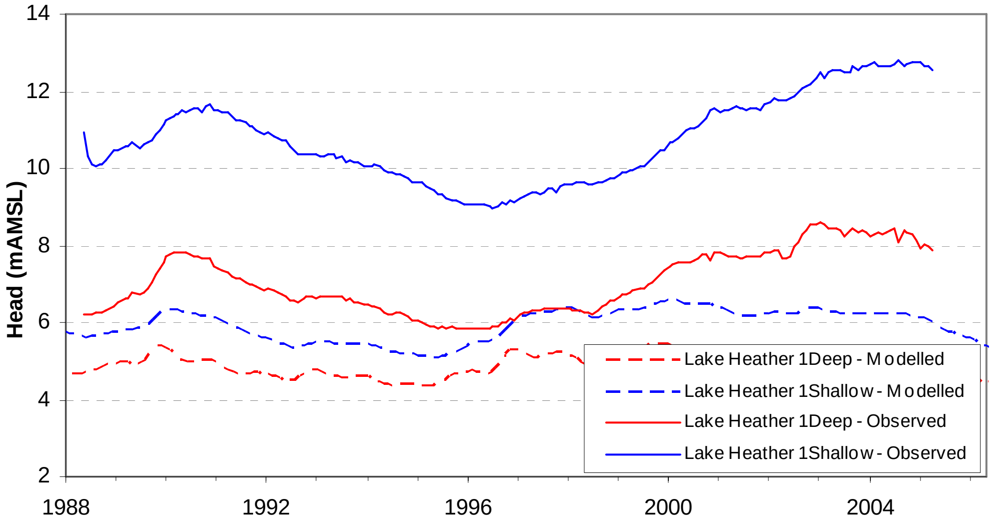

Figure 21. Modelled and observed heads at Lake Heather bores for sensitivity analysis scenario 1 (100% increased K).

Figure 22 demonstrates the sensitivity of heads in the alluvial plain to doubled hydraulic conductivity. This shows a distinct decrease in the seasonal variability in head and an approximate 1 m drop in average head.

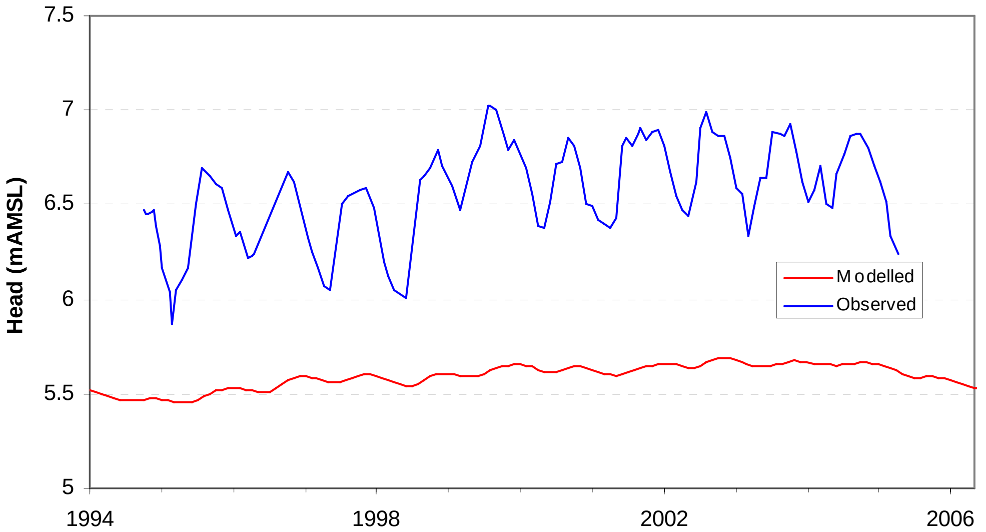

- **Figure 22. Modelled and observed heads at Crene bore for sensitivity analysis scenario 1 (100% increased K).**

4.4.2 Scenario 2: 50% decrease in K

In this scenario, sensitivity is tested to a 50% decrease in hydraulic conductivity across the whole model. Table 6 provides horizontal hydraulic conductivity values used in this analysis. Vertical hydraulic conductivity is determined by the anisotropy factor specified in Table 3.

- **Table 6. Hydraulic conductivity (K) values used for sensitivity analysis scenario 2.**

Material ID	K_h (m/d)	K_h (m/s)
Loose dunesand	5	5.8e-5
Weathered dunesand	3	3.5e-5
Fine sand	1.5	1.7e-5
Peat and sand	0.05	5.8e-7
Upper alluvium	0.275	3.2e-6
Alluvium	0.03	3.5e-7
Shell bed	25	2.9e-4

The effect of 50% reduction in model K values on calibration in the dunes (Lake Heather bores) is shown in Figure 23. A 4 – 10 m approximate increase in average heads is observed, as well as an increase in variability. The level of vertical confinement has also increased due to the scaling effect of the anisotropy factor.

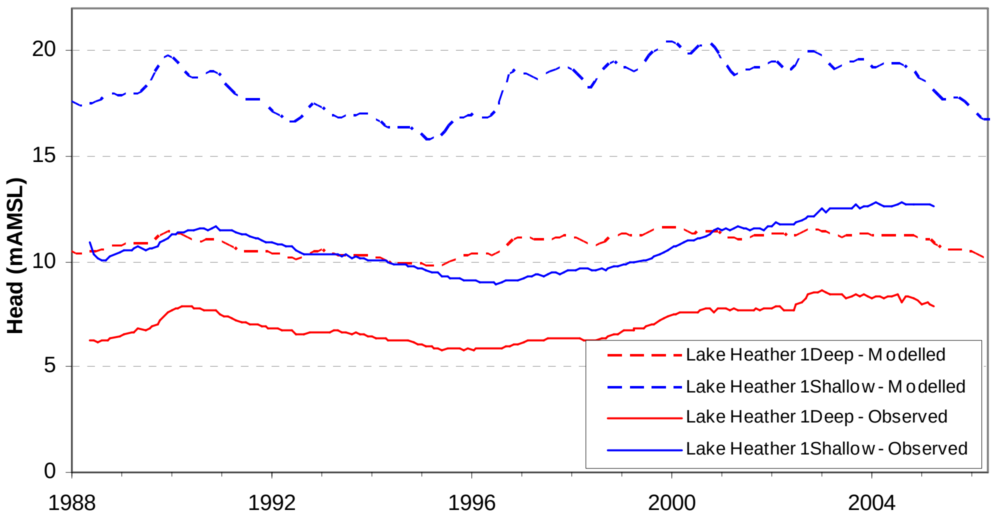

- **Figure 23. Modelled and observed heads at Lake Heather bores for sensitivity analysis scenario 2 (50% decreased K).**

Similarly, at the Crene bore on the alluvial plain, modelled seasonal variability and mean head have increased compared to calibrated results. Average modelled head is 1.25 to 2 m greater than observed values (Figure 24).

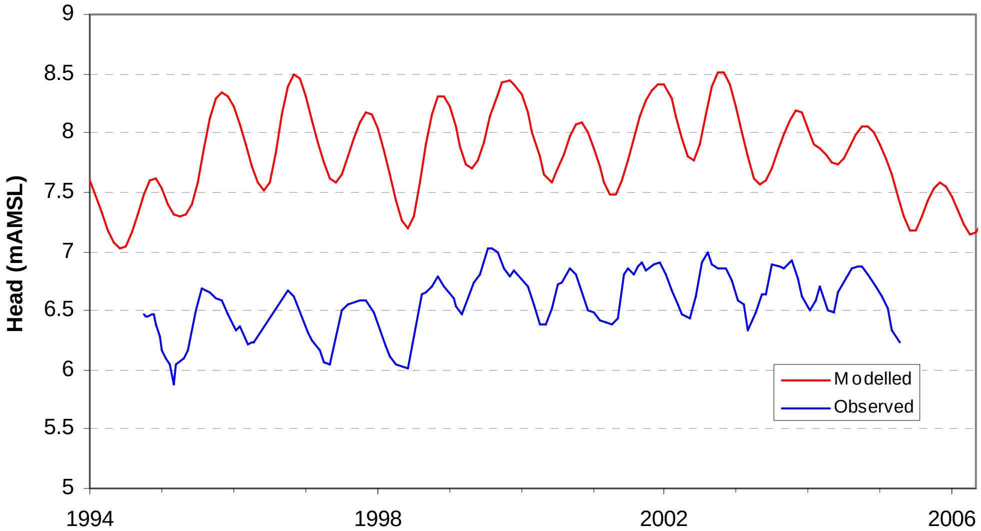

- **Figure 24. Modelled and observed heads at Crene bore for sensitivity analysis scenario 2 (50% decreased K).**

4.4.3 Summary

Overall, model calibration is sensitive to changes in hydraulic conductivity and provides a best representation of the system given the limitations in data availability.

5. Predictive Simulations

5.1 Setup

Predictive model simulations were carried out over a 50-year timeframe from 1957 to 2007. This allowed direct comparison to be made to calibrated model outputs and provided an adequate timeframe for equilibration to the simulated scenarios. These simulations are intended to assess relative responses in groundwater dynamics and groundwater level changes resulting from the sealing of free flowing artesian bores. Quantification of predicted changes should therefore be considered indicative only.

The following three scenarios were simulated and compared to calibrated model outputs:

- ***Scenario 1:*** Instant closure of artesian bores. Following an initial period of five years after simulation commencement, all free flowing artesian bores are capped in January 1962.
- ***Scenario 2:*** 10 year progressive artesian bore closure. Beginning January 1962 in the model simulation, blocks of artesian bores will be closed so that the final block of bores are closed in January 1972.
- ***Scenario 3:*** 30 year progressive artesian bore closure. Beginning January 1962 in the model simulation, blocks of artesian bores will be closed so that the final block of bores are closed in January 1992.

The three scenarios detailed above are depicted in Figure 25 below, which shows timeframes implemented for bore closure under each scenario. The stepped nature of the plot denotes the progressive closure of eleven blocks of bores (each block containing 9 or 10 bores) with either 1 or 3 year intervals for Scenarios 2 and 3 respectively. Blocks of bores were closed in a relatively random order, but consistently between the compared scenarios.

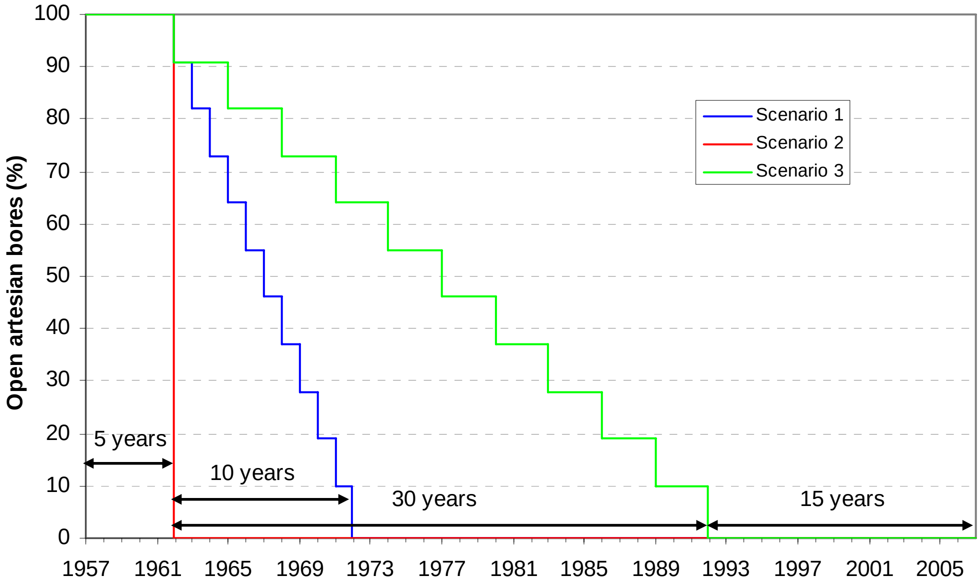

- **Figure 25. Progressive bore closure schedule implemented for predictive simulations.**

5.2 Results

The following sections describe the results of predictive simulations for each scenario for the following:

- transient groundwater levels;
- piezometric surfaces, and;
- flow budgets.

The results below provide an indication of the likely response to bore closure had it been implemented historically. Due to uncertainties in artesian flow characteristics and limitations in model calibration, the magnitude of predicted changes is indicative only focuses on relative responses.

5.2.1 Transient Groundwater Levels

This section investigates the effects of each prediction scenario on groundwater oscillatory responses at various zones within the model domain. The three locations assessed are shown in Figure 26 and are as follows:

- ***Zone 1:*** Within the shell bed (Layer 4) in the centre of the plains. This zone is expected to have the most significant impact from bore closure, as it is the aquifer from which most of the artesian bores drain.

- ***Zone 2:*** Within model Layer 1 near the centre of the dune ridge. This zone is likely to experience a less significant change from capping of artesian bores.
- ***Zone 3:*** Within model Layer 1 on the alluvial plains. This location is expected to be impacted to some degree by artesian bore closure due to a localised response to reduced drawdown however vertical confinement is expected to dampen these impacts.

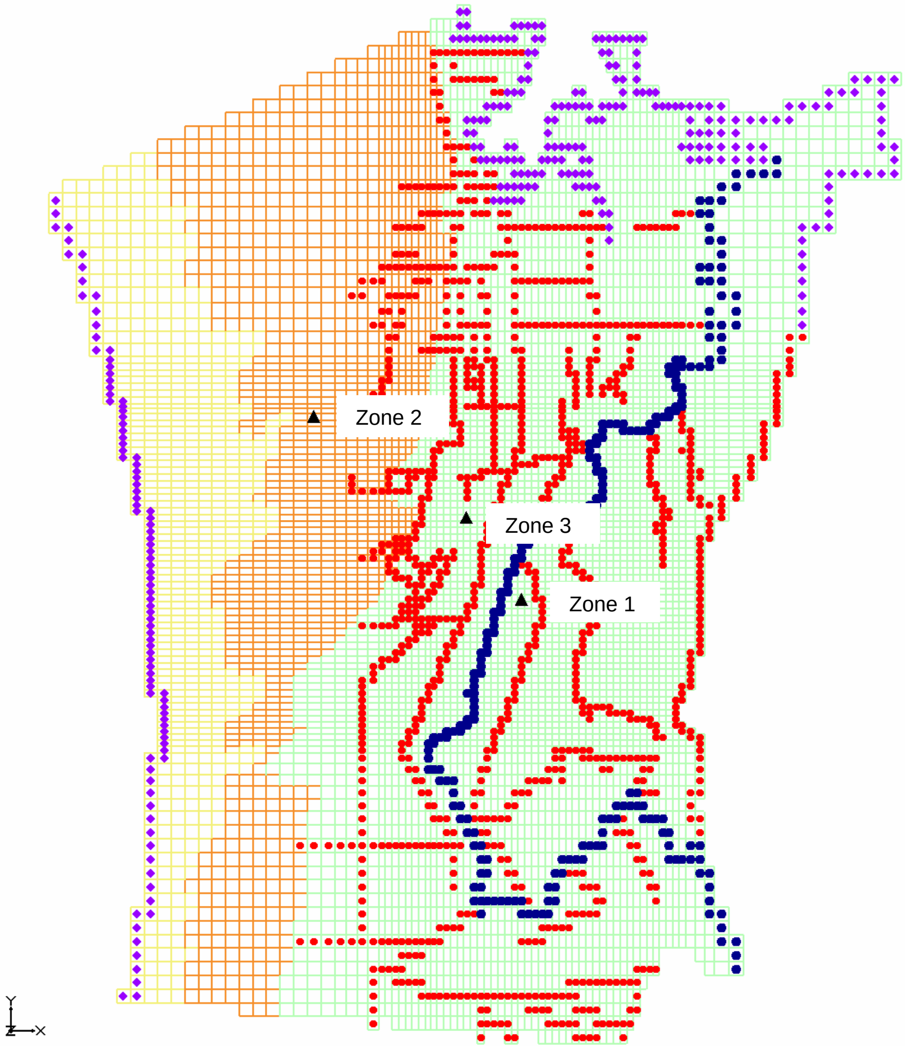

Figure 26. Map showing the locations of each zone used for hydrograph comparison.

Zone 1 – Shell bed:

Groundwater hydrographs for the three prediction scenarios and the calibrated model are presented in Figure 27. The indicative total change in pressure head resulting from capping all free flowing artesian bores (calculated by subtracting status quo from predicted transient heads) is

SKM

approximately 1 m (Figure 28), corresponding to 156% of the modelled natural fluctuation at this location. The scenarios show that several years following complete closure in all schemes, the total simulated effect on the aquifer is identical. However, the rate of change brought about by each scenario closely matches the timeline of bore closure. This suggests that as expected, the shell bed aquifer from which the artesian bores drain responds very quickly to these changes while full equalisation of pressures across the entire aquifer system takes a significantly longer period. Following bore closure, the aquifer also shows a greater sensitivity to recharge, signified by a larger degree of head fluctuation.

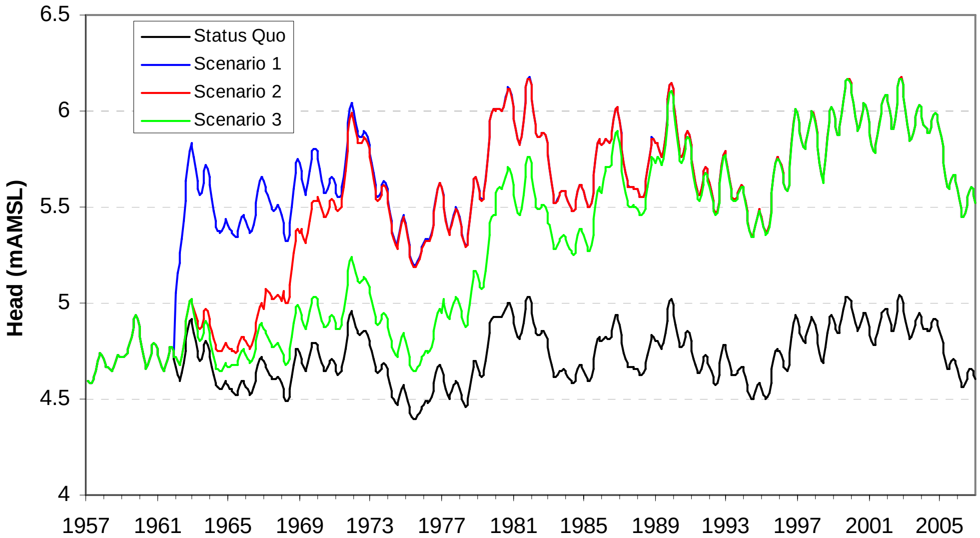

- **Figure 27. Simulated groundwater hydrographs for prediction scenarios within the shell bed aquifer (Zone 1).**

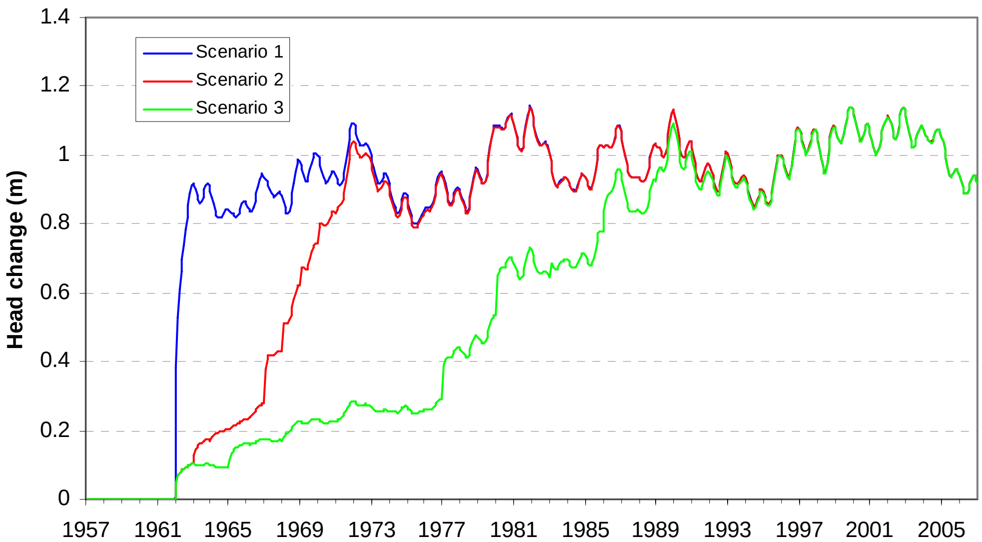

SKM

- **Figure 28. Pressure head changes from calibrated model within the shell bed aquifer (Zone 1) for various prediction scenarios.**

Zone 2 – Dune ridge:

The groundwater hydrographs for Zone 2 situated in the top model layer in the centre of the dune ridge are shown in Figure 29 and the head differences are plotted in Figure 30. At this location, the potential maximum increase in head brought about by bore closure is 0.42 m, which accounts for 15% of the 2.7 m range of calibrated model heads. While the indicative total head change is nearly half a metre, the impact of bore closure is much less when compared to natural fluctuations at this location. A delay in response is also noted when compared to Zone 1. The horizontal distance of this site from the zone of extraction as well as the vertical layer separation are responsible for this delay.

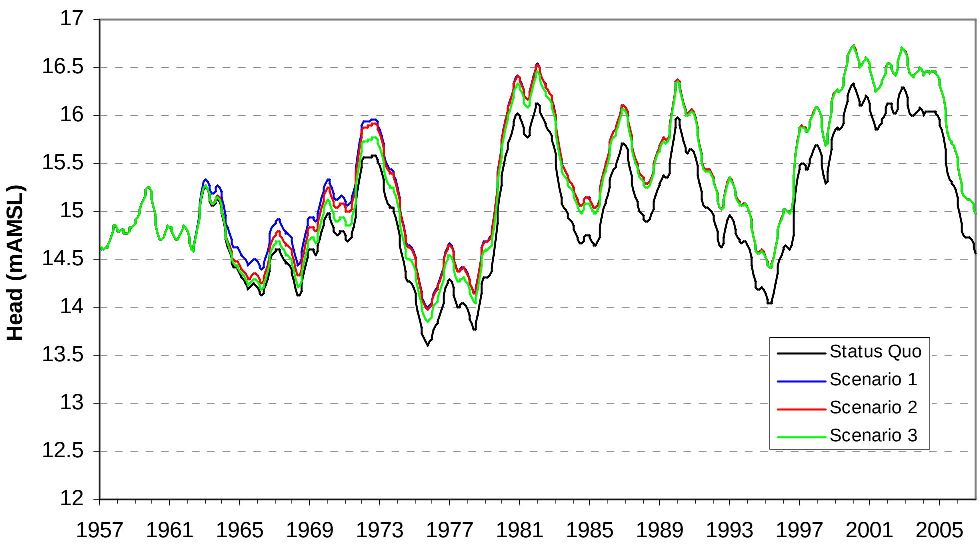

- **Figure 29. Simulated groundwater hydrographs for prediction scenarios within the dune ridge (Zone 1).**

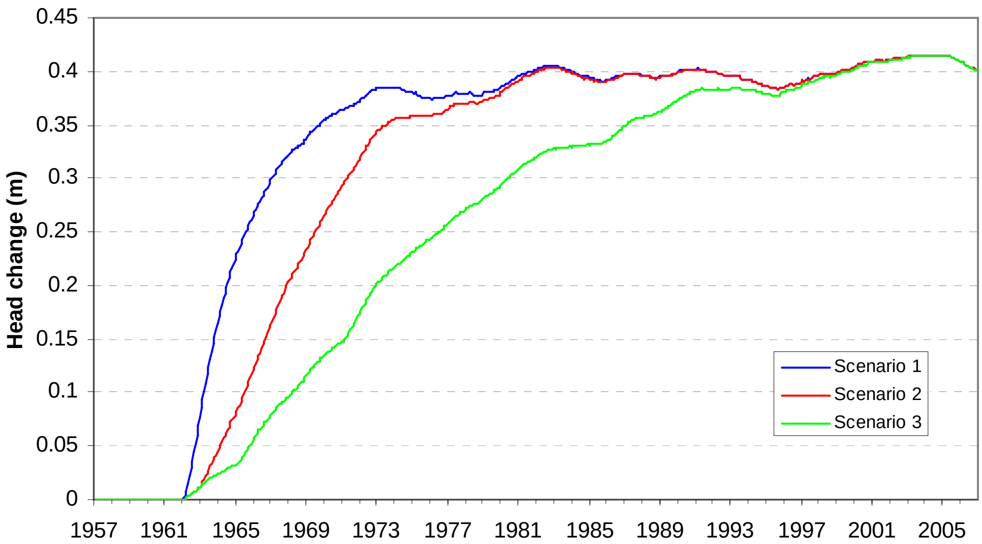

- **Figure 30. Pressure head changes from calibrated model within the dune ridge (Zone 2) for various prediction scenarios.**

Zone 3 – Upper alluvial plain:

Potential effects of bore closure scenarios to surface layer heads in the alluvial plain are shown in Figure 31 and Figure 32. The indicative maximum modelled head increase at this site is 0.75 m corresponding to 61% of the modelled range in natural fluctuations. This increase is significant in the unconfined aquifer, considering that the water table is already fairly shallow, and may lead to ground saturation. While the direct impact on this zone is less than for Zone 1, the rate of change is very similar and no significant delayed response is noted.

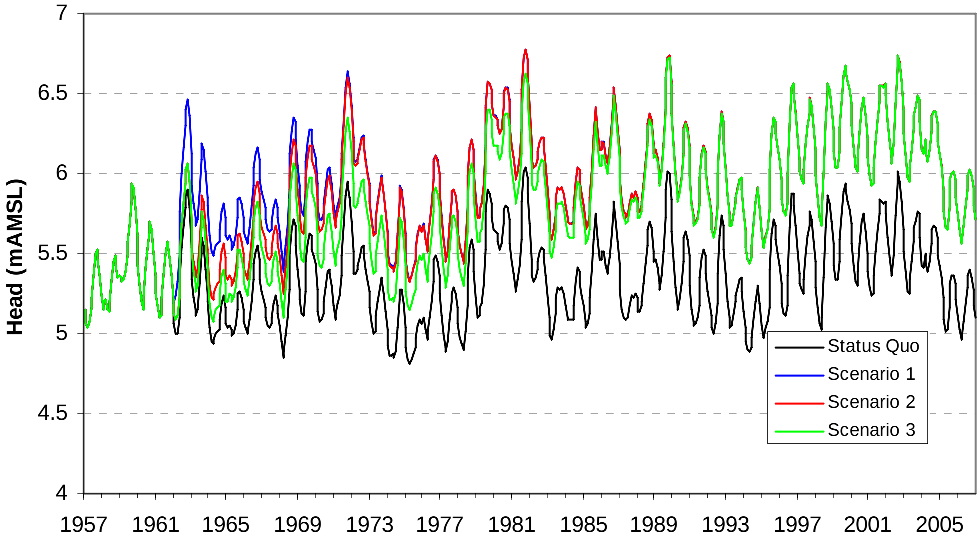

- **Figure 31. Simulated groundwater hydrographs for prediction scenarios within the upper alluvial plain (Zone 3).**

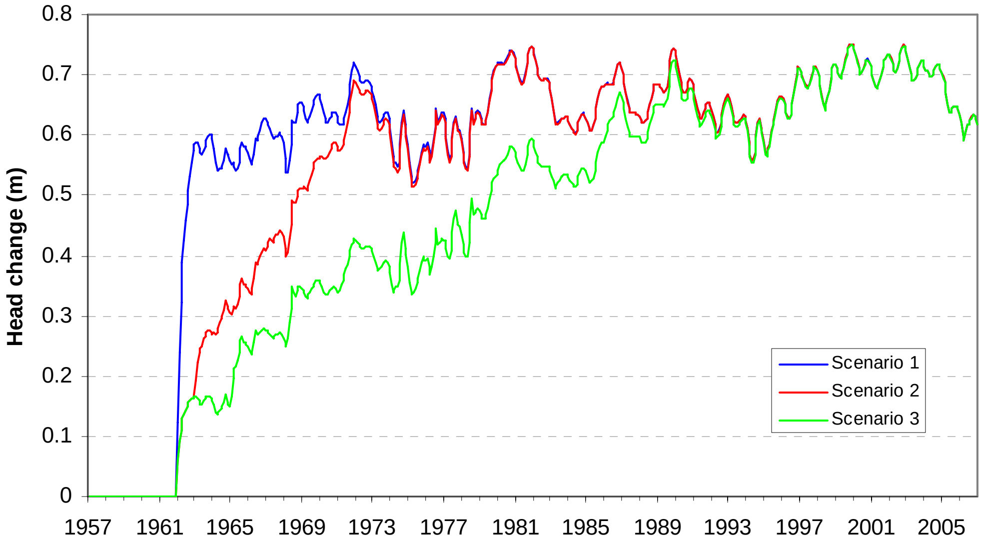

- **Figure 32. Pressure head changes from calibrated model within the upper alluvial plain (Zone 3) for various prediction scenarios.**

5.2.2 Piezometric Surfaces

This section describes the indicative effects of bore closure in terms of the piezometric surface geometry within the model domain. The end time step of the model is examined and comparison is not made between the three scenarios as their effects on pressure heads at this point are the same (see previous section).

The calibrated piezometric surfaces for each model layer are shown in Figure 33. Areas of higher head are shaded in lighter blue. The overall trend is of a diverging ridge of piezometric pressure along the sand dunes and flow migrating in the general direction of the Rangaunu Harbour and towards the coast to the west as per Section 4.3.1. These piezometric surfaces form the basis of comparison for complete artesian bore closure.

- **Figure 33. December 2006 calibrated model piezometric surfaces.**

  (See A3 attachment at rear).

Modelled piezometric heads for the same time step as above but with complete closure of flowing artesian bores are presented in Figure 34. The same overall flow pattern exists, however some degree of head increase is observed.

- **Figure 34. December 2006 model piezometric surfaces following closure of all flowing artesian bores.**

  (See A3 attachment at rear).

Figure 35 presents the indicative total change in head between Figure 33 and Figure 34 and shows the modelled degree of head change in each model layer. The most significant changes occur in the bottom two model layers, which experience a potential maximum head increase of over 1.5 m.

- **Figure 35. December 2006 modelled head difference (m) induced by closure of all flowing artesian bores.**

  (See A3 attachment at rear).

The zone of maximum modelled head increase coincides with the zone of maximum modelled artesian pressures (Figure 36). The zone of artesian pressures does not increase significantly in area following bore closure. However, the magnitude of artesian pressure adjacent to the base of the dunes is increased.

- **Figure 36. Extent of artesian pressures in model Layer 4 for a) status quo and b) capping of artesian bores.**

  (See A3 attachment at rear).

5.2.3 Flow Budgets

By closing flowing artesian bores, it is expected that some increase in other flow components will occur. This section assesses the modelled impacts to these flow budget components with particular focus on flows to the coast (constant head boundaries), drains and to the Awanui River. Increased flow to drains is of particular interest as it may have impacts on the ability of drains to mitigate surface flooding.

Figure 37 shows the modelled change in flow from the model to artesian bores, constant head boundaries, river and drains for prediction scenario 3 (30 year progressive bore closure). Artesian flow is reduced to zero in this scenario by 1992 (i.e. flow change in Figure 37 of -5,000 m^3/d). After this point, the indicative maximum increase in flow to coastal constant head boundaries is 1,800 m^3/d and the indicative maximum increase in the flow to drains and the river are 3,300 and 467 m^3/d respectively.

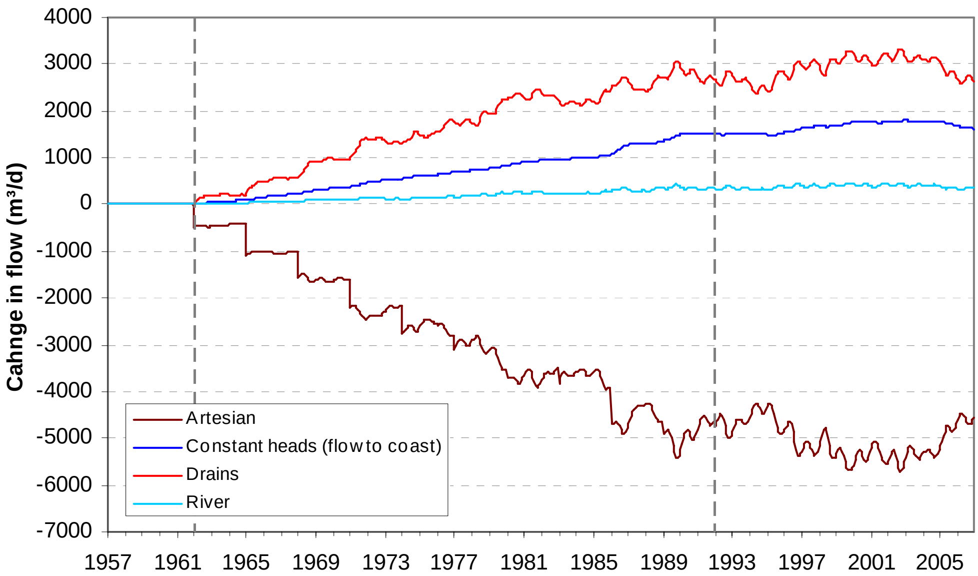

- **Figure 37. Modelled change in flow budget components from 30 year progressive bore closure (Scenario 3). Vertical lines denote closure period.**

Figure 38 presents the above information in terms of a percentage change to each component of flow. The greatest percentage increase in flow is experienced by the river (maximum 20% increase) due to its relatively small contribution to the flow budget. It should be noted that this corresponds to the increase in flow to the river from within the model domain only and will be a small component of total river flow which comes mainly from outside the model boundary. Drain flows experience a maximum 16% increase compared to a 3.4% maximum increase to flows to constant head boundaries.

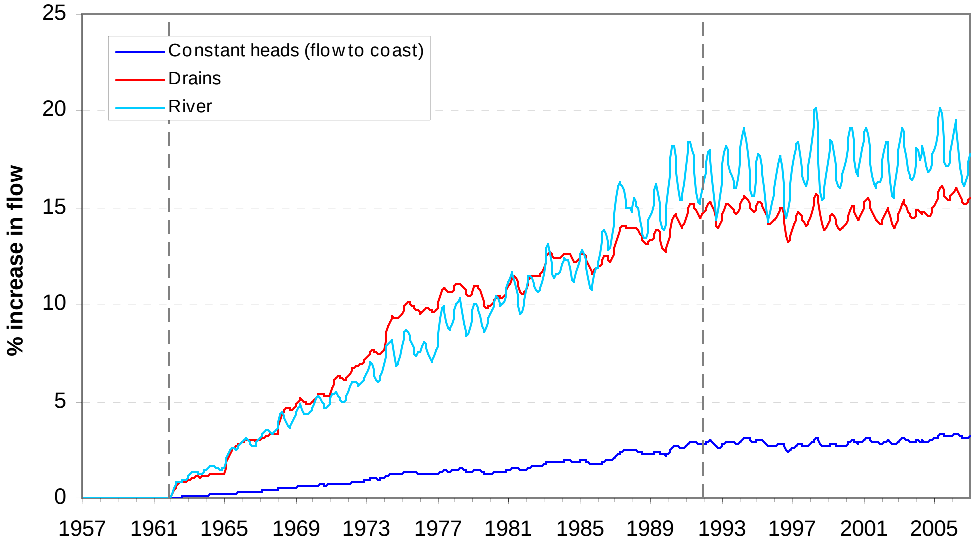

- **Figure 38. Percentage modelled increase to flow budget components from 30 year progressive bore closure (Scenario 3). Vertical lines denote closure period.**

A stabilised mean flow budget is summarised in Table 7 comparing status quo and artesian bore closure scenarios. The flow budget is averaged across the last forty years of the model period so that an assessment can be made of the flow budget once the hydrogeological system has had a chance to fully equilibrate to artesian bore closure. Model inflows remain very similar, however outflows increase to balance the reduction in artesian bore drainage.

- **Table 7. Modelled mean flow budgets for stabilised period (1967 – 2007) following artesian bore closure.**

Component	Flow In (m^3/day)		Flow Out (m^3/day)	
	Status quo	Scenario 1	Status quo	Scenario 1
Net change in storage	167	119	0	0
Constant heads	0	0	-56,427	-58,054
Drains	n/a	n/a	-19,125	-21,954
Artesian bores	n/a	n/a	-4,895	0
Rivers	115	100	-2,192	-2,568
Recharge	82,357	82,357	n/a	n/a
TOTAL FLOW	**82,640**	**82,576**	**-82,640**	**-82,576**

*Flow values indicative only due to model uncertainty.

Assuming that all free flowing artesian bores ultimately discharge into the surface drainage network, an assessment can be made to determine the net impact on drain flows from capping artesian bores. By adding drain flows and artesian bore discharge for each scenario, it can be seen that indicative average modelled net drain flows are 21,317 and 21,954 m^3/d for status quo and bore closure respectively. This equates to a negligible increase, suggesting that the only impacts on the flow budget will be minor increases in flows to the coast and to the Awanui River.

5.2.4 Summary of Results

Predictive model simulations to test the likely effects of artesian bore capping offered the following findings:

- Impacts to groundwater pressures were greatest in the shell bed and alluvial plain deposits and model hydrographs showed a quick response to bore closure;
- Groundwater levels in the dune formation had a less significant and more delayed response to bore closure;
- The maximum modelled head increase due to bore closure occurred in the artesian aquifer on the alluvial plain near Awanui;
- If it is assumed that artesian bores discharge into the existing drainage network, closure will have limited impacts on longterm drain flows, and;
- Closure of existing free flowing bores will increase groundwater outflows to the coast.

6. Conclusions

The key objectives of this study were to develop a groundwater MODFLOW model to characterise the hydrogeological system in the Awanui area and use it to simulate the likely effects of artesian bore closure. A four layer MODFLOW 2000 model was developed and was calibrated to the available transient water level data. The calibrated model showed that:

- Recharge to the model area occurs predominantly in the dune sands;
- Progressive confinement of groundwater in the alluvial plain due to low permeability estuarine sediments means that artesian pressures are generated in the underlying shell and sand formation, and;
- Most of the recharge that occurs in the dunes flows to the west coast. The proportion that flows east into the artesian aquifer and direct recharge to the plains are discharged (in order of decreasing magnitude) to drains, flowing artesian bores, the Rangaunu Harbour and the Awanui River.

Three scenarios of the calibrated model were utilised to determine the relative impact of the immediate or progressive closure of free flowing artesian bores. Comparison of these predictive simulations indicated that:

- increased flow to surface water features due to bore closure will be balanced by the fact that these bores will no longer discharge to drains;
- the magnitude and speed of pressure rise in the groundwater system were greatest in close proximity to the zone of the existing free flowing bores and least further away (e.g. in the dune zone);
- due to the fast groundwater response to closure, the order in which bores are progressively capped will have little difference on aquifer impacts. Likewise, the time period over which bores are closed will define the period of aquifer response;
- an increase in groundwater flow to the coast will result from artesian bore closure, and;
- capping of flowing artesian bores will make more groundwater available for legitimate users and increase water use efficiency in the area.

Overall, the modelling undertaken indicates that closure of free flowing bores will result in increased heads in the sand and shell aquifer reverting them to ‘near-natural’ conditions. Response to bore closure is expected to be immediate in the confined aquifer, so the rate of head recovery depends on the programme of works. Due to the expected speed of response, the order in which bores are closed is not likely to have a significant effect on the resulting impacts. Flows in the drains are not expected to change significantly due to bore closure and these are not likely to impact on flood risk.

Currently, the flowing artesian bores in the Awanui Plain release a significant degree of pressure from the shell and sand aquifers and closure of these bores will inevitably lead to increased heads in the groundwater system and a potentially higher water table elevation. The implications of this may be that the prevalence of surface ponding and soil saturation will increase due to a diminished buffering storage capacity in the unconfined aquifer. Accordingly, the management of bore closure works should consider these potential effects, particularly in the area around Awanui where the model shows the largest pressure response.

6.1 Model Limitations

In interpreting the conclusions drawn from the scenario modelling, the degree of uncertainty in model results due to limitations in the available data should be considered. Limitations to the model conceptualisation process were identified in SKM (2006) and include the following:

- The limited amount of data available to define aquifer hydraulic parameters;
- Spatial and temporal resolution of groundwater level monitoring data;
- Reliability and consistency amongst drillers geological logs;
- The unknown number and flow of open artesian bores in the area, and;
- The unknown number and flow of pumped abstraction from groundwater.

7. References

HydroGeo Solutions, 2000. Aupouri Aquifer Sustainable Yield Groundwater Modelling Study. Report prepared for Northland Regional Council.

Pitman W.V., 1976. A Mathematical Model for Gnerating Daily River Flows from Meteorological Data in South Africa. Joint CSIR – University Council Hydrological Research Unit, South Africa.

Sinclair Knight Merz, 2006. Awanui Artesian Aquifer Conceptualisation. Report prepared for Northland Regional Council.

Appendix A Recharge Modelling

The soil moisture water balance model (SMWBM) is a deterministic lumped parameter model originally developed by Pitman (1976) to simulate river flows in South Africa. Modification of these algorithms and reworking of the code into a Windows environment now permits soil moisture accounting and assessment of the various components of the catchment water balance. In this study, the model is used to determine the percolation to groundwater component of the water balance to be applied directly as aquifer recharge to the groundwater model.

The model utilised the rainfall record for Kaitaia from 1987 to 2006 (period of continuous data) and mean monthly potential evaporation at the same location. No sufficient stream flow records were available to calibrate the model, however knowledge of the hydrogeology and previous modelling work enabled realistic soil characteristic parameters to be set. Dome degree of calibration in the groundwater model allowed additional parameterisation of the water balance model.

The model operates on a maximum timestep of daily during dry days, with smaller timesteps (hourly) implemented on wet days. When a rainday occurs, daily rainfall is disaggregated into the hourly timesteps based on a pre-defined synthetic rainfall distribution, which includes peak intensities during the middle of the storm. The model time stepping ensures that rainfall intensity effects and antecedent catchment conditions are considered in a realistic manner.

The model utilises daily rainfall and mean-monthly evaporation data to calculate soil moisture conditions and rainfall percolation to the aquifer. The model incorporates parameters that characterise the catchment in terms of:

- interception storage,
- evaporation losses,
- soil moisture storage capacity,
- soil infiltration rates,
- soil moisture percolation rates;
- surface runoff (quickflow);
- stream baseflows (groundwater contribution); and
- parameters that govern the recession and/or attenuation of groundwater and surface water flow components, respectively.

The fundamental operation of the model is as follows:

SKM

Daily rainfall is disaggregated into hourly intervals when a rainday occurs to allow refined accounting of soil infiltration and evaporation losses. Rainfall received must first fill a nominal interception storage (PI – see below) before reaching the soil zone, where the net rainfall is assessed as part of the runoff/infiltration calculation.

Water that penetrates the soil fills a nominal soil moisture storage zone (ST). This zone is subject to evapotranspiration via root uptake and direct evaporation (R) according to the mean monthly evaporation rate and current soil moisture deficits. The soil moisture zone provides a source of water for deeper percolation to the underlying aquifer, which is governed by the parameters FT and POW.

If disaggregated hourly rainfall is of greater intensity than the calculated hourly infiltration rate (ZMAX, ZMIN) surface runoff occurs. Surface runoff is also governed by two other factors, which are the prevailing soil moisture deficit and the proportion of impervious portions of the catchment directly linked to drainage pathways (AI).

Rainfall of sufficient intensity and duration to fill the soil moisture storage results in excess rainfall that is allocated to either surface runoff or groundwater percolation depending on the soakage and slope characteristics of the catchment (DIV).

Finally, the model produces daily summaries of the various components of the catchment water balance and calculates the combined surface runoff/percolation to groundwater to form a total catchment runoff discharge.

A.1 Model Parameters

ST: Soil thickness

ST defines the size of the soil moisture store in terms of a depth of water.

SL: Soil moisture storage capacity below which percolation ceases

There is a definable soil moisture state below which percolation ceases due to soil moisture retention. For practical purposes this has been assigned zero.

ZMAX & ZMIN: Maximum and minimum soil infiltration rate

ZMAX and ZMIN are nominal maximum and minimum infiltration rates in mm/hr used by the model to calculate the actual infiltration rate ZACT. ZMAX and ZMIN regulate the volume of water entering soil moisture storage and the resulting surface runoff. ZMIN is usually assigned zero. ZMAX is usually assigned the saturated infiltration rate from field testing. ZACT may be greater than ZMAX at the start of a rainfall event. ZACT is usually nearest to ZMAX when soil moisture is nearing maximum capacity.

FT: Percolation rate from soil moisture storage at full capacity

Together with POW, FT (mm/day) controls the rate of percolation to the underlying aquifer system from the soil moisture storage zone. FT is the maximum rate of percolation through the soil zone.

POW: Power of the soil moisture-percolation equation

The parameter POW determines the rate at which percolation diminishes as the soil moisture content is decreased. POW therefore has significant effect on the seasonal distribution and reliability of percolation, as well as the total yield from a catchment.

AI: Impervious portion of catchment

This parameter represents the proportion of impervious zones of the catchment directly linked to drainage pathways (AI).

R: Evaporation-soil moisture relationship

Together with the soil moisture storage parameters ST and SL, R governs the evaporative process within the model. The rate of evapotranspiration is estimated using a linear relationship relating evaporation to the soil moisture status of the soil. As the soil moisture capacity approaches full, evaporation occurs at a near maximum rate based on the mean monthly pan evaporation rate, and as the soil moisture capacity decreases, evaporation decreases linearly according to the predefined function.

DIV: Fraction of excess rainfall allocated directly to groundwater.

DIV has values 0 – 1 and defines the fraction of excess (ponded) water due to saturation of the soil zone to be routed to groundwater or surface water.

TL: Routing coefficient for surface runoff.

TL defines the lag of surface water runoff. This is not necessary to define for this study as we are only interested in the groundwater percolation component of the water balance.

GL: Groundwater recession parameter.

Has no effect in this application of the model as we are only interested in percolation to groundwater, not the discharge of groundwater to surface water bodies.

Two unique recharge zones were defined based on surface geology for the western dune sands and alluvial plain deposits. Each zone has parameters defined that reflect the soil characteristics and rainfall response behaviour for each geology type. Final model parameters for each are provided in Table A1.

- **Table A1. SMWBM model parameters used for recharge estimation.**

Zone	ST (mm)	Z_{MAX} (mm/hr)	FT (mm/d)	POW	AI	R	DIV
Dunes	1000	30	2.5	2	0	0	0.5
Plains	500	5	0.3	2	0.01	0	0

A.2 Model Results

Water balance partitioning for the two zones are presented in Table A2. The primary difference in water balance partitioning between the two zones is that water is preferentially routed to surface runoff on the alluvial plain and to groundwater in the dune zone. The maximum soil and infiltration rates (ZMAX and FT respectively) are the key parameters responsible for this difference, attributable to the contrasting hydraulic properties of the dune sands and floodplain sediments. Groundwater percolation data used for groundwater model recharge is presented in Figure 4 (Section 2.2.2).

- **Table A2. Modelled water balance partitioning (%).**

Zone	Interception	Soil Evaporation	Surface Runoff	Groundwater Percolation
Dunes	32	30	2	36
Plains	22	37	37	4

Appendix B Model Boundary Elevations